Site-Specific Modification of Gold Nanoparticles by Underpotential Deposition of Cadmium Atoms

Gabriel J. Gordillo[1], Silvana A. Ramírez[2] and Mathias Brust[3]*

[1] Departamento de Química Inorgánica, Analítica y Química Física, Facultad de Ciencias Exactas y Naturales, INQUIMAE (CONICET), Universidad de Buenos Aires, Ciudad Universitaria, Pabellón 2 (1428), Buenos Aires, Argentina.

[2]Area Química, Instituto de Ciencias, Universidad Nacional de General Sarmiento. J.M.Gutierrez 1150 (1613). Los Polvorines, Prov. de Buenos Aires. Argentina.

[3] Department of Chemistry, University of Liverpool, Crown Street, Liverpool L69 7ZD, United Kingdom.

Corresponding Author

*Gabriel Gordillo gabriel@qi.fcen.uba.ar

ABSTRACT. Underpotential deposition (UPD) of cadmium on 15 *nm* gold nanoparticles stabilised by 1-mercapto-undecane-11-tetra(ethyleneglycol) and adsorbed to a hanging mercury drop electrode (HMDE) has been studied by cyclic voltammetry. It is shown that single cadmium atoms are deposited onto the same surface sites that, in the absence of cadmium, are active for adsorptive hydrogen reduction. Depending on the pH of the solution, the deposition of cadmium atoms either blocks hydrogen reduction or vice versa, according to which process occurs first during the cathodic potential sweep.

TOC GRAPHICS

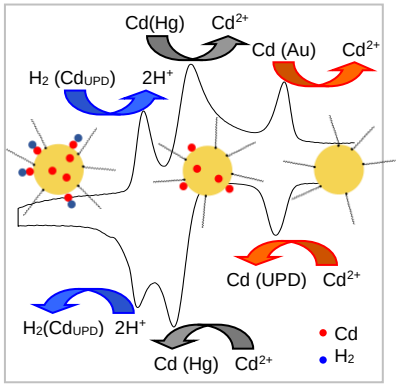

KEYWORDS. Electrochemistry, Catalysis, Nanotechnology, Proton Reduction, Hanging Mercury Drop Electrode

Following the groundbreaking work in the early 1990s by Haruta, Hutchings, Goodman and others on the catalytic activity of supported gold nanoparticles[1-7], gold has since become one of the most intensely studied elements in heterogeneous catalysis research. While bulk gold is known to be chemically inert, it has by now been amply demonstrated that gold nanoparticles, supported and unsupported, ligand-stabilised or not, can be highly active both as oxidation, and as reduction catalysts[7-8]. Given the current practical interest in solar energy conversion, batteries and fuel cells, research in electrocatalysis by gold nanoparticles is also blossoming.[9-11]

Electrochemical studies on nanoparticles invariantly require contacting the particles with a working electrode[12], either by diffusion from a dispersion of particles, or, more commonly, by attaching the particles to the electrode surface. This usually leads to a convoluted electrochemical signal from the nanoparticles, and from the surface of the working electrode in addition to complications that can arise from interactions between densely packed particles. Hutchinson *et al.* have recently shown that boron doped diamond is a good electrode material to study immobilized gold nanoparticles without much interference from the base electrode[13]. They also showed that the electrochemical signal of a redox active moiety attached to the nanoparticles becomes clearer and sharper when the particles are individually tethered to the electrode and are well separated from each other. Another exceptionally good substrate for nanoparticle electrochemistry is the hanging mercury drop electrode (HMDE), which behaves like a pure capacitor over a large potential range and thus permits the study of electrochemical processes on adsorbed particles only. Presumably due to the liquid nature of the substrate, the nanoparticles interfere spatially very little with each other and give a voltammetric response of unrivalled quality. The HMDE thus represents an excellent experimental platform for the detailed electrochemical investigation of electrocatalytic processes at nanoparticles.

We have recently demonstrated electrocatalytic adsorptive hydrogen ion reduction on thiolate-capped gold nanoparticles adsorbed to an HMDE[14]. This process differs markedly from hydrogen evolution on bulk gold electrodes, which requires a more negative potential and does not lead to adsorbed molecular hydrogen. The thiolate ligand shell does not passivate the particles but permits access of protons to a determined number of highly active sites on the metal surface. Hydrogen ions adsorb to these sites and are electrocatalytically reduced at zero over potential.

Electrochemical metal deposition on bulk gold electrodes protected by thiol SAMs has been shown before [15-20]. Usually the newly deposited metal lodges under the SAM. Given the curvature of nanoparticles, it can thus be assumed that access of ionic or small molecular redox species to the metal surface is generally also possible. The characteristic electrochemical signature of hydrogen ion reduction on these particles in contact with a HMDE has also been used to probe the penetration of a phospholipid monolayer by gold nanoparticles. This could be relevant for assessing the ability of nanoparticles to cross biological membranes[21].

Here we report that the same sites active for hydrogen reduction are also active for the under potential deposition (UPD) of cadmium and that, depending on the experimental conditions only one of the two processes takes place and blocks the respective other. The robustness and reproducibility of this quite intricate self-assembled electrochemical system is remarkable and the interpretation and analysis of all results is straightforward. While UPD of cadmium on bulk gold electrodes is a well-studied phenomenon[22-25], there are relatively few reports on UPD on metal nanoparticles. Crooks and co-workers primed noble metal nanoparticles by copper UPD for subsequent galvanic replacement and also investigated metal deposition on dendrimer encapsulated noble metal nanoparticles [26-29], Kumar and Buttry reported UPD of copper on

palladium nanoparticles[30], and Campbell and Compton deposited lead and cadmium on an array of silver nanoparticles[31].

In Figure 1, cyclic voltammograms of 15 nm PEG-thiolate-capped gold nanoparticles (PEG-Au nps) adsorbed to a HMDE before and after the addition of cadmium nitrate are shown. Before the addition, the only feature of the voltammogram is the adsorptive reduction and oxidation of hydrogen ions at a potential of -0.225 V (peaks 1).

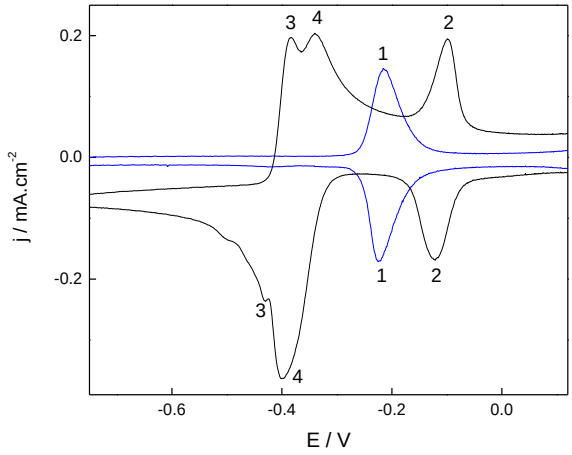

Figure 1. Cyclic voltammetric response of a dispersion of 15 nm gold nanoparticles (40 nM) at a hanging mercury drop electrode in aqueous acetic acetate buffer (0.1M, pH 4.5) in the absence of cadmium (blue line) and after Cd(II) addition (black line, 0.11mM final concentration). Scan rate: 1 Vs-1. Potentials are quoted against NHE.

This was reported earlier for 3 and 15 nm gold nanoparticles with the same thiol capping [14]. Both particle sizes had a discrete number of active sites for this process with a significantly higher proportion of sites in the smaller particles. By simple scaling, it is possible to estimate that the same process also occurs on bulk gold electrodes but is never seen in real measurements due to the overwhelmingly large capacitive component and the vanishingly small proportion of active sites.

Once a sufficient amount of cadmium has been added, this hydrogen peak disappears, and instead a new peak of identical height and shape appears at -0.123 V. Unlike the hydrogen reduction peak that shifts accordingly with pH, this new peak is pH independent. In addition, a double peak appears in the region around -0.384 V. We interpret these changes as the suppression of hydrogen reduction by the more anodically occurring under potential deposition (UPD) of cadmium atoms on the active sites (peaks 2). The new double peak is readily identifiable as a combination of the diffusionally controlled reduction and amalgamation of cadmium on the proportion of the mercury electrode that is not covered with particles (peaks 4), and adsorptive hydrogen evolution on the deposits of cadmium on the gold nanoparticles (peaks 3). The peak resulting from cadmium reduction on mercury in the absence of gold nanoparticles (see S.I.1) is identical with the more anodic part of the double peak, which confirms our assignment. When this peak is subtracted from the voltammogram, the remaining feature strongly resembles the cadmium UPD peak (S.I.2) but its position depends on the pH value of the electrolyte solution and shifts by 54 mV per pH unit, typical for a 2-electron 2-proton reduction process (S.I.3). Therefore its assignment as adsorptive hydrogen reduction on the cadmium deposits on the active sites of the gold nanoparticles is justified.

As the HMDE becomes increasingly covered with gold nanoparticles the diffusionally controlled cadmium reduction and amalgamation on the free mercury surface becomes highly irreversible and is finally almost completely suppressed (S.I.4). All other measurements were carried out under conditions where the nanoparticles only occupy a small proportion of the electrode surface. This is directly evidenced by an environmental SEM study of a mercury surface under a thin film of water containing the nanoparticles at comparable concentration (Figure 2). As soon as the liquid water disappears, while a high relative humidity is maintained to keep the particles

hydrated, islands of adsorbed particles can clearly be seen. At higher resolution, the individual particles are resolved and can also be found outside the islands freely dispersed on the mercury surface. The near perfectly spherical islands are likely to be drying patterns that form when the thin water film breaks up. They are probably not present under the conditions of the electrochemical experiments. It is also important to note that the particles disappear quickly as the electron beam is scanned across them. Under those conditions they probably lose some ligands and then amalgamate with the mercury electrode. This is a limitation that impedes a more detailed electron microscopic study of this system.

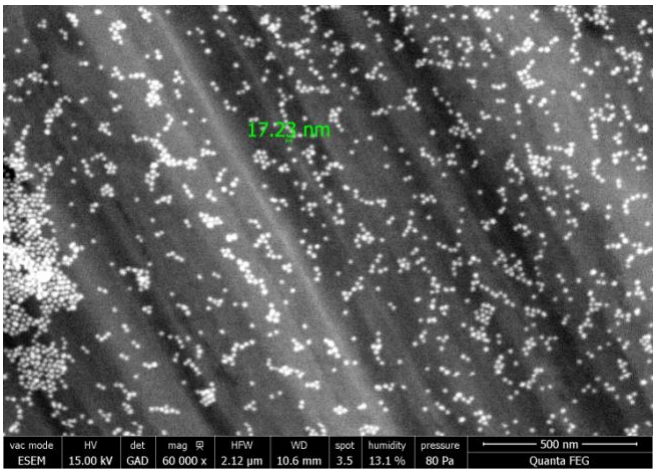

Figure 2. 15kV Backscattered electron image in ESEM mode showing Au nanoparticles, here of *ca.*17 nm in diameter, adsorbed on a mercury surface.

We have identified three different electrochemical processes that occur at the active sites of the adsorbed gold nanoparticles. The first one is hydrogen reduction in the absence of cadmium, the second is UPD of cadmium and the third hydrogen reduction on the cadmium deposits. Notably, the same amount of charge transfer is associated with each of the three processes. This is illustrated in Figure 1 for hydrogen reduction in the absence of cadmium and UPD of cadmium, and in Figure 3 a and b for UPD of cadmium and hydrogen reduction on cadmium. In Figure 3a,

cyclic voltammograms are presented at different times, during the gradually occurring adsorption of gold nanoparticles to the HMDE in the presence of a sufficient amount of cadmium ions. The peaks corresponding to UPD of cadmium and those corresponding to hydrogen reduction on the cadmium deposits grow simultaneously and identically with time (figure 3b) , while the peak corresponding to cadmium reduction on the free mercury surface remains practically constant and only depends on the cadmium concentration (as long as the coverage of the HMDE with nanoparticles remains low).

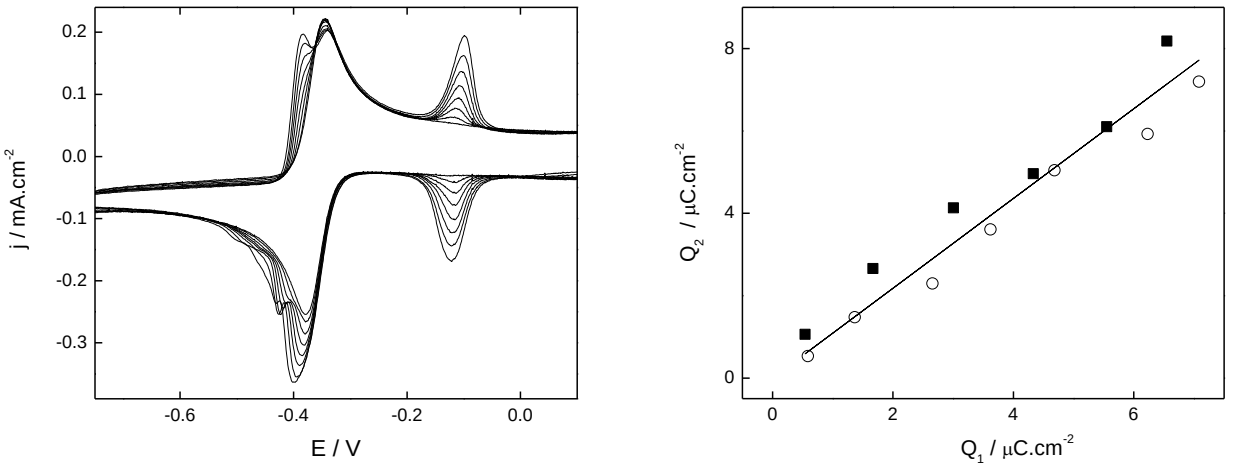

Figure 3. a) Cyclic voltammograms recorded during nanoparticles adsorption on mercury in the presence of Cd(II). Conditions are indicated in figure 1. b) Comparison of charges involved in the H+/H2 couple on deposited Cd (Q2) and the charge involved in the cadmium UPD (Q1) for cathodic (■) and the anodic (○) processes. Charges were calculated from the data in figure 3a. The slope equals 1.09.

The exact replacement of the hydrogen reduction peak with the cadmium UPD peak and the fact that each process requires the transfer of two electrons are strong indications that the three processes occur at the same surface sites of the gold nanoparticles and that cadmium is deposited as single adatoms per site.

An interesting situation shown in Figure 4 is obtained at pH 2, where, due to the shift of the hydrogen reduction potential the UPD of cadmium on the active sites would occur at more cathodic potentials than hydrogen reduction. In this case, these sites are always blocked with adsorbed hydrogen, which completely suppresses the UPD. We speculate that these active sites consist of isolated planes made from three close packed gold atoms, *i.e*. embryonic Au111 faces without interconnectivity. On each 15 nm particle, we assume the presence of ca. 130 sites [14] to which access of ions and small molecules is not obstructed by the thiol ligands. This is also consistent with the, for gold, unusual adsorptive 2 electron hydrogen reduction since there is no surface diffusion and hence no combination of colliding hydrogen atoms. Each site is therefore responsible for the reductive production of one hydrogen molecule or one cadmium adatom, respectively. The sites for UPD of cadmium on bulk Au111 surfaces have been determined by Bondos *et al.* using electrochemical scanning probe microscopy[25].

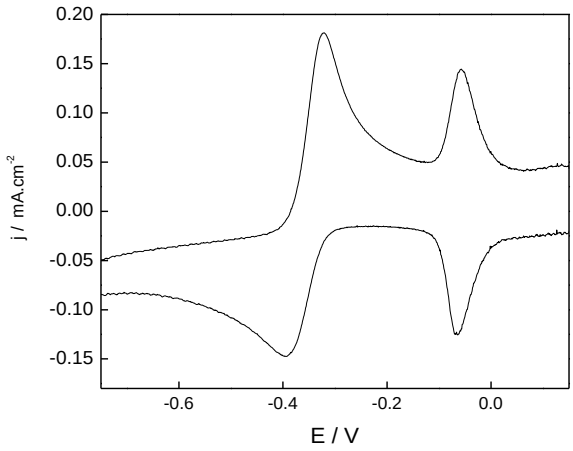

Figure 4. Cyclic voltammetric response of a dispersion of 15 nm gold nanoparticles (40 nM) at a hanging mercury drop in the presence of 0.11 mM Cd(II) (pH 2): Scan rate 1 Vs^{-1} .

They reported the formation of adatoms on all available sites, *i.e*. two-fold, three-fold hollow and atop sites. Attempting here to unequivocally identify the active sites on the nanoparticles thus remains speculative since cadmium quite readily seems to deposit on any site available. The highly reproducible and clean electrochemical behaviour of the particles does however suggest that all sites involved are equivalent. We have preliminary evidence that these sites are also active for the UPD of copper (see S.I.5) but not of zinc, cobalt or nickel. Hydrogen reduction on the copper adatoms occurs at less cathodic potentials with respect to cadmium adatoms.

What remains to be clarified is what we mean by a sufficient amount of cadmium. This is at least enough cadmium to form a deposit on each hydrogen reduction site on the gold nanoparticles to suppress electrocatalytic hydrogen reduction on this site. If the cadmium concentration is too low, not all active sites on the gold particles are covered with cadmium, and hydrogen reduction occurs both on the remaining active sites, and at more cathodic potential, at the sites covered with cadmium (see S.I.6). Under such condition, the system evolves a more complex electrochemical behaviour that is not subject of the present study but may later become of interest for cadmium trace analysis. Here, we either worked in the absence of cadmium or in the presence of an amount sufficient to cover all UPD/hydrogen reduction sites on the gold nanoparticles.

In summary, we have presented a detailed and conclusive electrochemical study of the deposition of cadmium adatoms on ligand-capped gold nanoparticles and the correspondent changes in the particle's hydrogen electrochemistry. Processes that occur in parallel on the mercury support electrode, *i.e.* capacitive charging and diffusionally controlled reduction and amalgamation of cadmium, can easily be completely separated from the processes occurring on the nanoparticles. These particles have a discrete number of identical sites that are accessible and highly active for

either adsorptive hydrogen ion reduction or under potential metal atom deposition. These processes mutually exclude each other, however, hydrogen reduction takes place also on deposited atoms albeit at much more cathodic potential. The HMDE represents an ideal tool to establish electrochemical contact to nanoparticles initially dispersed in the electrolyte solution and to investigate their electrochemical reactivity with high precision and high reproducibility. Here is has been possible to self-assemble an active electrode that contained only one type of electrochemically active sites resulting in highly reproducible and clean voltammogams. We believe that our studies will stimulate more research on site-specific electrochemical processes on a range of nanoparticles of different metals, in particular in view of gaining detailed information on site-specific electrocatalysis in mixed metal clusters.

EXPERIMENTAL METHODS

Gold nanoparticles were prepared by an established in-house variant of the Turkevich-Frens method[14]. Particle stability and dispersibility in water was achieved by the choice of mercapto-undecane-11-tetra(ethyleneglycol) as a ligand. Nanoparticles dimension and concentration were determined according to Haiss *et al.* [32].

For the electrochemical characterization, the nanoparticles were added as aqueous dispersions to the corresponding pH buffer that also served as supporting electrolyte: acetate buffer solution (0.1 M, pH 4.75), sodium borate (0.1 M, pH 9.2), phosphate buffer (0.1 M, pH 7.0). In the case of the experiments performed at pH 2.0, enough HNO_3 (conc) was added to a 0.1M KNO_3 solution.

A freshly generated hanging mercury drop served as working electrode, which was polarized with respect to Ag|AgCl 3.5 M reference electrode using a platinum wire as counter electrode.

A 1000 ppm Cd(II) standard solution was used to prepare Cd(II) solutions used in all the experiments.

The SEM micrographs were recorded with a FEI Quanta FEG Environmental Scanning Electron Microscope (ESEM) equipped with a Peltier cooled stage. A peltier cooled sample holder was used to image specimen in the natural state or in "wet" mode. Samples for inspection by environmental scanning electron microscopy (Fei-ESEM) were prepared by depositing a droplet (typically ca. 10 µL) of mercury withing a depression in a stainless steel sample holder and covering it with a thin aqueous film of nanoparticle dispersion (1-2 µL). As the film is slowly evaporated under controlled pressure in the microscope the individual gold nanoparticles adsorbed to the mercury surface become visible.

Supporting_Information:

SI 1: peak resulting from cadmium reduction on mercury in the absence of gold nanoparticles.

SI 2: subtracted voltammogram.

SI 3: Dependence of peak potentials on pH.

SI 4: Suppression of the diffusionally controlled cadmium reduction and amalgamation on the free mercury surface due to the high coverage of gold nanoparticles.

SI 5: Copper UPD.

SI 6: Effect of low Cd(II) concentration.

Author information

Corresponding Author

*gabriel@qi.fcen.uba.ar

ACKNOWLEDGMENTS

Financial support from UBACYT (20020120100281BA) and PIP Nº 1142-01101-00421 (CONICET) is gratefully acknowledged. Silvana Ramírez acknowledges Universidad Nacional de General Sarmiento for support. GJG is member of the research career of CONICET, Argentina. Mathias Brust acknowledges support from the European Research Council under the European Union's Seventh Framework Programme (FP7/2007-2013) / ERC-Advanced Grant project 321172 PANDORA.

REFERENCES

(1) Haruta, M.; Tsubota, S.; Kobayashi, T.; Kageyama, H.; Genet, M. J.; Delmon, B. Low-Temperature Oxidation of CO over Gold Supported on TiO_2, α-Fe_2O_3, and Co_3O_4. *J. Catal.* **1993**, *144*, 175-192.

(2) Valden, M.; Lai, X.; Goodman, D.W. Onset of Catalytic Activity of Gold Clusters on Titania with the Appearance of Nonmetallic Properties. *Science* **1998**, *281*, 1647-1650.

(3) Torres Sanchez, R. M.; Ueda, A.; Tanaka, K.; Haruta, M. Selective Oxidation of CO in Hydrogen over Gold Supported on Manganese Oxides. *J. Catal*. **1997**, *168*, 125–127.

(4) Rainer, D. R.; Xu, C.; Goodman, D.W. Characterization and catalysis studies of small metal particles on planar model oxide supports. *J. Mol. Catal. A* **1997**, *119*, 307-325.

(5) Nkosi, B.; Adams, M. D.; Coville, N. J.; Hutchings, G. J. Hydrochlorination of acetylene using carbon-supported gold catalysts: A study of catalyst reactivation. *J. Catal.* **1991**, *128*, 378-386.

(6) Nkosi, B.; Coville, N. J.; Hutchings, G. J.; Adams, M. D.; Friedl, J.; Wagner, F.E. Hydrochlorination of acetylene using gold catalysts: A study of catalyst deactivation. *J. Catal.* **1991**, *128*, 366-377.

(7) Hutchings, G. J.; Catalysis: A golden future. *Gold Bulletin* **1996**, *29*, 123–130.

(8) Zhang, Y.; Cui, X.; Shi, F.; Deng, Y. Nano-Gold Catalysis in Fine Chemical Synthesis. *Chem. Rev*. **2012**, *112*, 2467–2505.

(9) Mirkhalaf, F.; Schiffrin, D.J. Electrocatalytic Oxygen Reduction on Functionalized Gold Nanoparticles Incorporated in a Hydrophobic Environment. *Langmuir* **2010**, *26* (18), 14995–15001.

(10) Yan, S.; Zhang, S.; Lin, Y.; Liu; G. Electrocatalytic Performance of Gold Nanoparticles Supported on Activated Carbon for Methanol Oxidation in Alkaline Solution. *J. Phys. Chem. C* **2011**, *115* (14), 6986–6993.

(11) Kamat, P.V. Photophysical, Photochemical and Photocatalytic Aspects of Metal Nanoparticles. *J. Phys. Chem. B* **2002**, *106*, 7729-7744.

(12) Murray, R.W. Nanoelectrochemistry: Metal Nanoparticles, Nanoelectrodes, and Nanopores. *Chem. Rev*. **2008**, *108*, 2688–2720.

(13) Young, S.L.; Kellon, J.E.; Hutchison, J.E. Small Gold Nanoparticles Interfaced to Electrodes through Molecular Linkers: A Platform to Enhance Electron Transfer and Increase Electrochemically Active Surface Area. *J. Am. Chem. Soc*. **2016**, *138*, 13975–13984.

(14) Brust, M; Gordillo, G.J. Electrocatalytic Hydrogen Redox Chemistry on Gold Nanoparticles. *J. Am. Chem. Soc*. **2012**, *134*, 3318–3321.

(15) Manolova, M.; Ivanova, V.; Kolb, D.M.; Boyen, H.G.; Ziemann,P.; Büttner, M.; Romanyuk, A.; Oelhafen, P. Metal deposition onto thiol-covered gold: Platinum on a 4-mercaptopyridine SAM. *Surface Science* **2005,** *590*, 146–153.

(16) Ivanova, V.; Baunach, T.; Kolb, D.M. Metal deposition onto a thiol-covered gold surface: A new approach. *Electrochimica Acta* **2005**, *50*, 4283-4288.

(17) Oyamatsu, D.; Kuwabata, S.; Yoneyam, H. Underpotential deposition behavior of metals onto gold electrodes coated with self-assembled monolayers of alkanethiols.. *Journal of Electroanalytical Chemistry* **1999**, *473*, 59–67.

(18) Jennings, G.K.; Laibinis, P.E. Self-Assembled n-Alkanethiolate Monolayers on Underpotentially Deposited Adlayers of Silver and Copper on Gold. *J. Am. Chem. Soc*.**1997**, *119*, 5208–5214.

(19) Schneeweiss, M.A.; Hagenström, H.; Esplandiu, M.J.; Kolb, D.M. Electrolytic metal deposition onto chemically modified electrodes.. *Applied Physics A* **1999,** *69*, 537–551.

(20) Oyamatsu, D.; Nishizawa, M.; Kuwabata, S.; Yoneyama, H. Underpotential Deposition of Silver onto Gold Substrates Covered with Self-Assembled Monolayers of Alkanethiols To Induce Intervention of the Silver between the Monolayer and the Gold Substrate. *Langmuir* **1998**, *14*, 3298–3302.

(21) Gordillo, G.J.; Krpetic, Z.; Brust, M. Interactions of Gold Nanoparticles with a Phospholipid Monolayer Membrane on Mercury. *ACS Nano* **2014**, *8*, 6074–6080.

(22) Ge, M.H.; Gewirth, A.A. In situ atomic force microscopy of under- and overpotentially deposited cadmium on Cu(111) *Surface Science* **1995,** *324*, 140-148.

(23) Niece, B.K.; Gewirth, A.A, Potential-Step Chronocoulometric and Quartz Crystal Microbalance Investigation of Coadsorbed Cadmium and Sulfate on Au(111) Electrodes. *Langmuir* **1997**, *13*, 6302–6309.

(24) Hsieh, S.-J. Gewirth, A. Nitrate Reduction Catalyzed by Underpotentially Deposited Cd on Au(111): Identification of the Electroactive Surface Structure. *Langmuir* **2000**, *16*, 9501–9542.

(25) Bondos, J.C.; Gewirth, A.A.; Nuzzo, R.G. Observation of Uniaxial Structures of Underpotentially Deposited Cadmium on Au(111) with in Situ Scanning Tunneling Microscopy. *J. Phys. Chem*. **1996**, *100*, 8617–8620.

(26) Carino, E.V.; Crooks, R.M. Characterization of Pt@Cu Core@Shell Dendrimer-Encapsulated Nanoparticles Synthesized by Cu Under-potential Deposition. *Langmuir* **2011**, *27*, 4227–4235.

(27) Yancey, D.F.; Carino, E.V.; Crooks, R.M. Electro-chemical Synthesis and Electrocatalytic Properties of Au@Pt Dendrimer-Encapsulated Nanoparticles. *J. Am. Chem. Soc*. **201**0, *132*, 10988–10989.

(28) Carino, E.V.; Kim, H.Y.; Henkelman, G; Crooks, R.M Site-Selective Cu Deposition on Pt Dendrimer-Encapsulated Nanoparticles: Correlation of Theory and Experiment. *J. Am. Chem. Soc.* **2012**, *134*, 4153-4162.

(29) Knecht, M.R; Weir, M.G.; Myers, V.S; Pyrz, W.D.; Ye, H; Petkov, V; Buttrey, D.J.; Frenkel, A.I; Crooks, R.M. Synthesis and Characterization of Pt Dendrimer-Encapsulated Nanoparticles: Effect of the Template on Nanoparticle Formation. *Chem. Mater*. **2008**, *20*, 5218-5228.

(30) Kumar, A.; Buttry, D.A. Size-Dependent Underpotential Deposition of Copper on Palladium Nanoparticles. *J. Phys. Chem. C* **2015**, *119*, 16927–16933.

(31) Campbell, F.W.; Compton, R.G. Contrasting Underpotential Depositions of Lead and Cadmium on Silver Macroelectrodes and Silver Nanoparticle Electrode Arrays. *Int. J. Electrochem. Sci.* **2010**, *5*, 407 – 413.

(32) Haiss, W.; Thanh, N.T.K; Aveyard, J.; Fernig, D.G. Determination of Size and Concentration of Gold Nano-particles from UV-Vis Spectra. *Anal. Chem*. **2007**, *79*, 4215-4221.

.